Application of a Phenomenological Soot Model to Diesel Engine Combustion

A.Fusco, A.L.Knox-Kelecy* and D.E.Foster*
CNR, Naples
Italy
* *University of Wisconsin-Madison*

ABSTRACT

A phenomenological soot model has been used to simulate soot production for combustion conditions typical of a diesel engine. The model accounts for the number of carbon atoms in the fuel and incorporates the physical processes of inception, surface growth, coagulation, and oxidation using global rate expressions. It consists of four differential equations balancing the rates of change of particle number density, soot precursor radicals, acetylene (assumed to be the soot growth species), and soot volume fraction. Arrhenius type global kinetic rate expressions have been written for most of the processes considered. For a few of the processes, such as coagulation and oxidation, detailed rate expressions of non-Arrhenius form have been taken from the literature. The model has been coded in FORTRAN and is operational as a stand-alone sub-model. It has been used to simulate soot production using inputs of fuel, oxygen, temperature and pressure profiles based on results obtained from a KIVA II simulation of a Cummins diesel engine. The model has demonstrated the ability to handle a wide range of temperatures in both rich and lean mixtures with predictions that behave as expected. Both the shapes and the magnitudes of the profiles for soot volume fraction, particle number density, soot precursor radicals, and acetylene growth species are predicted to behave consistently with the trends published in the literature.

INTRODUCTION

Diesel engines need to meet progressively stricter emission standards, thus further efforts are needed from researchers and manufacturers to decrease the emissions to lower values. In particular, soot emissions have been widely investigated and exhaustively reviewed in the current literature [1,2,3]. If successfully developed, an engineering soot model could be used as a powerful tool in the analysis and predictions of soot emissions from diesel engines.

Several models for soot formation and oxidation have been implemented for diesel engines. Hiroyasu [4] has reported the most widely used models from 1962 to 1984, which are essentially based on empirical formulas for predicting the formation and oxidation of soot particles. Some soot models, originally developed for premixed and diffusion flames, have been used in diesel engines. Zellat et al. [5] used the soot formation model of Tesner et al. [6] and the turbulent soot oxidation model of Magnussen et al. [7,8]. Another example is illustrated by Belardini et al. [9] who implemented a modified version of the soot model developed by Leung et al. [10] for a laminar non premixed flame. A very basic model developed for diesel engines was implemented by Nishida et al. [11,12] and Belardini et al. [13]. A recent improvement of this model which implemented the Nagle and Strickland-Constable formula [14] for soot particle oxidation has been tested by Paterson et al. [15]. In yet another approach Gorokhovski et al. [16] have assumed that soot is generated from a stable hydrocarbon intermediate species, typical in the ignition chemistry, and constructed a generic model along the lines of the Shell ignition model [17]

This paper presents the results of a new phenomenological soot model specifically targeted as a sub-model for incorporation into complex diesel combustion models. The model contains descriptions of the important fundamental processes which control the soot emission from the engine. Specifically, the paper presents predicted results from a parametric study of the model applied to the engine-like conditions of a representative computational cell predicted by KIVA-II.

NEW PHENOMENOLOGICAL SOOT MODEL

The soot model presented in this paper is a phenomenological model which incorporates via global rate expressions the physical processes of pyrolysis, inception, surface growth, coagulation and oxidation. These processes are shown schematically in Fig. 1 where a portion of the fuel is converted to soot precursor radicals, represented by R, (1), and growth species, assumed to be C_2H_2, (2) . Radicals and growth species are considered to be separate species; although they could be the same species, at least at the very beginning of the soot formation process. A portion of the

precursor radicals are oxidized, (3), and the rest are converted to soot particles, (5). The growth species (assumed to be C_2H_2) increase the mass of the soot particles, (6). Oxidation is also included in the model with an assumption that the oxidation does not affect the particle number density. The growth species (C_2H_2 molecules) can disappear and the soot particles can lose mass via oxidation, (4) and (7) respectively, and the number of soot particles can decrease due to coagulation with other soot particles, (8). Reactions (1) through (8) are used to provide a balance on four variables predicted by the model. These are the particle number density, N (cm^{-3}), the soot precursor radicals, R (mol cm^{-3}), the acetylene growth species, C_2H_2 (mol cm^{-3}) and the volume fraction of the soot, f_v (cm^3-soot/cm^3-mix) The resulting four governing differential equations solved by the model are given in Table A1. From the solution of these equations the particle number density and volume fraction can then be used to estimate an average particle diameter (under the assumption of monodispersed spherical soot particle).

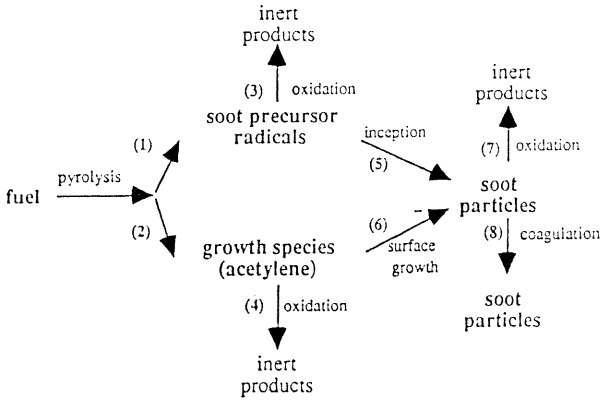

Figure 1. Schematic diagram of soot model processes

The rate constants for each of the global kinetic expressions were fit to be in the same range as similar types of reactions which have been detailed in the literature for elementary soot kinetic reactions. Table A2 gives a listing of the processes, chemical reactions, rate constants, activation energies and pre-exponential factors used in the model.

The model requires as input the time history of the temperature and fuel and molecular oxygen concentration. As output it predicts the time history of the soot particle number density, soot precursor radicals, soot growth species (acetylene) and soot volume fraction. It was originally tested and fit for a flame environment then without any further parameter adjustment it has been run for the engine-like conditions reported in this paper.

RESULTS AND DISCUSSION

The input data used were predicted by a KIVA-II simulation for a DI diesel engine. Specifically, a computational cell from a KIVA-II diesel simulation was chosen as being representative of conditions within the cylinder. Figure 2 shows the temperature, molecular oxygen and fuel concentrations as a function of crank angle (time) which were used as baseline input for the engine like conditions reported in this paper. The engine operating conditions and the KIVA-II simulation are reported in detail in Ref. [15]. With this input as a base condition a parametric study of the model was conducted in which the profiles of the temperature, oxygen or fuel concentrations shown in Figure 2 were multiplied by a constant; their time dependent shape was maintained, only the magnitude of the values was changed. All of the parameter variations were done without adjusting any of the model constants and with the assumption that there were 14 carbon atoms in the fuel molecule.

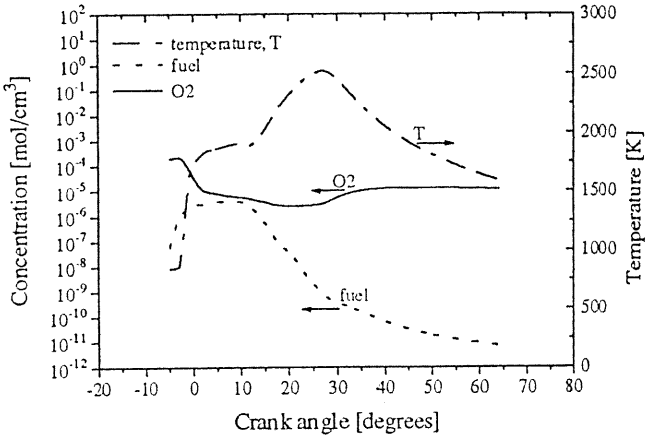

Figure 2. Temperature, oxygen and fuel profiles versus crank angle used as baseline input to the soot simulation model

Temperature Effect

Temperature influences both the formation and the oxidation of soot particles. All reaction rates are relatively sensitive to changes in temperature with the final net soot being controlled by a balance of the formation and oxidation of the soot particles. In the present model the soot formation is the net soot obtained from the balance of pyrolysis, inception, surface growth and gas phase oxidation.

The model's predicted temperature dependence of soot volume fraction is shown in Fig. 3. The labeling of the temperature profiles is accomplished by giving the peak value of the temperature. The shape of the temperature profile is like that shown in Fig. 2. The model predicts that both the formation and oxidation rates increase with increasing temperature. At lower temperatures the net soot volume fraction is controlled by the formation process, whereas the particle oxidation is not very large. Thus, soot is still present at the end of the residence time within the cylinder. In contrast, at higher temperatures soot particle oxidation becomes predominant even though the soot formation rate increases, as seen by the higher peak of soot volume fraction. The soot is completely burned out in the expansion stroke. A similar behavior has been observed by Kadota et al. [18] for a simulated diesel spray experiment.

They observed that the maximum of the soot concentration increased with an increase in the inlet air temperature, but the value at the exhaust decreased. Figure 3 also shows that the soot appears earlier as temperature increases. Finally, note that the model predicts that no soot would live through the expansion stroke for the base case, where the peak temperature is approximately 2500 K.

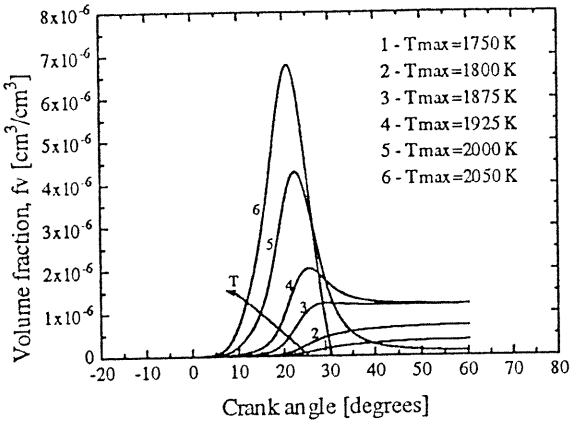

Figure 3. Predicted soot volume fraction versus crank angle as a function of peak temperature for temperature profiles as shown in Fig. 2.

Figure 4 shows the acetylene (growth species) concentrations predicted by the model at different temperatures. The acetylene concentration is controlled by the formation from the pyrolysis of the fuel, the oxidation by O_2 and the surface growth with soot particles. All these reaction rates increase with temperature, causing higher peak values of acetylene and lower concentrations at the end of the residence time.

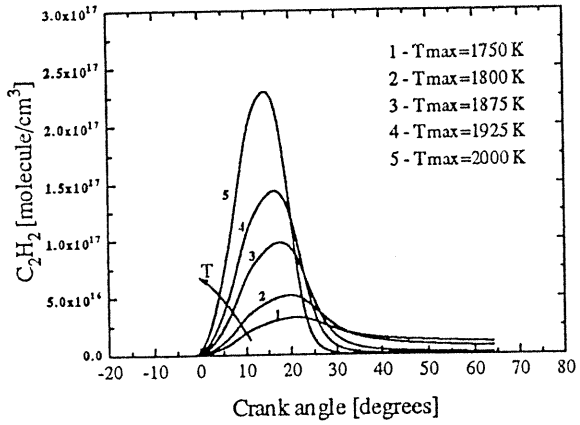

Figure 4. Predicted acetylene concentrations versus crank angle for different peak temperatures for temperature profiles shown in Fig 2.

Figure 4 also shows that acetylene peaks earlier with respect soot volume fraction (Fig. 3). The same behavior has been noted by Belardini et al. [13], who measured simultaneously both soot and acetylene in a diesel engine.

Figures 5 and 6 show the predicted temperature dependence of soot precursor radicals and soot number density profiles. Soot precursor radicals first appear and peak earlier than do the soot particles.

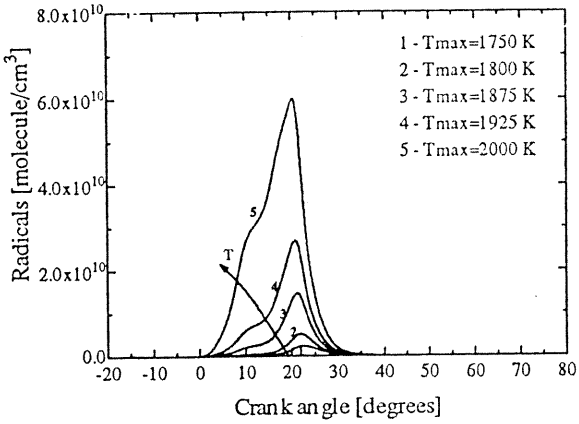

Figure 5. Predicted soot precursor radical concentration versus crank angle as a function of peak temperature for temperature profiles as shown in Fig. 2.

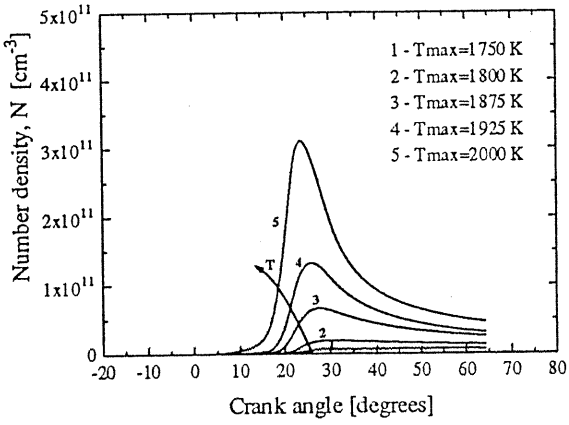

Figure 6. Predicted number density versus crank angle as a function of peak temperature for temperature profiles as shown in Fig. 2.

With an assumed monodispersed spherical particle distribution the particle number density and volume fraction were used to estimate an average particle diameter. Figure 7 shows the estimated diameter, at different temperatures, to be within the range measured in diesel engines [3,19], as well as those calculated by Smith [20]. Figure 7 also shows a decrease in the diameter with increasing temperature. This behavior agrees with the trend shown by Prado et al. [21] for carbon black.

The model has shown a rather strong temperature dependence on particle oxidation, which has been modeled according to the Nagle and Strickland-Constable formula

[14]. Figure 8 shows the comparison between soot volume fraction computed with and without the particle oxidation included. It can be noted that at lower temperatures the soot particle oxidation has a moderate effect on the soot volume fraction, whereas at higher temperatures the oxidation is effectively causing the complete burn out of the particles.

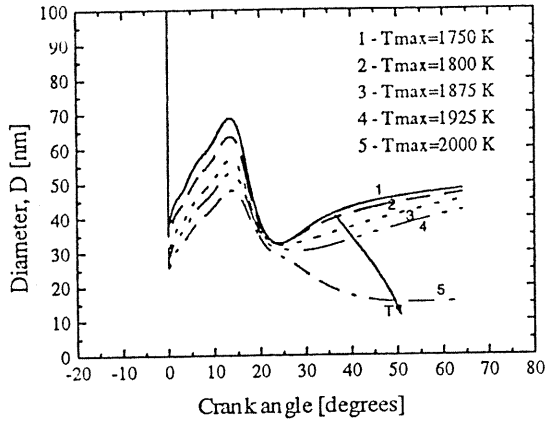

Figure 7. Predicted particle diameter versus crank angle as a function of peak temperature for temperature profiles as shown in Fig. 2.

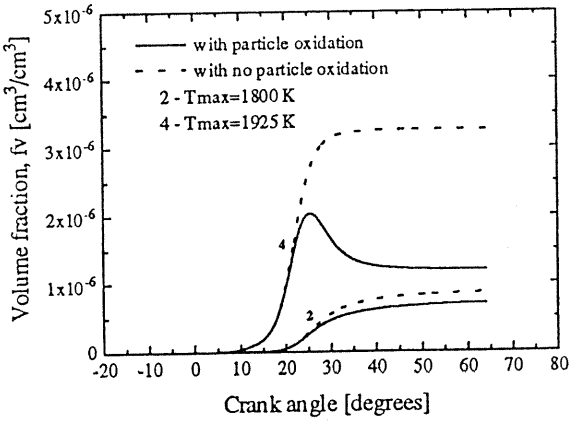

Figure 8. Demonstration of the effect of oxidation on predicted volume fraction for two different temperature profiles

Oxygen Effect

Figure 9 shows the oxygen dependence of the soot volume fraction. A single temperature profile, with a peak temperature of 2000 K, was used and the oxygen profile was scaled by a factor of one hundred below and above the original baseline. At lower oxygen concentrations the fuel-air mixture is rather rich, thus the oxidation of soot particles does not occur. On the contrary, soot particle oxidation becomes significant for leaner mixtures.

For the cases 1,2 and 3 of Fig. 9 the soot volume fraction was only influenced by the oxidation of the soot particles, whereas for cases 4 and 5 it was also influenced by the oxidation of the gas phase species. This assessment is apparent by observing the predicted acetylene concentrations for these five cases, as shown in Fig. 10. The figure shows that at the lower oxygen concentration of cases 1, 2 and 3 the gas phase oxidation does not occur, thus the oxygen dependence observed for these cases in Fig. 9 is only due to particle oxidation. On the contrary, gas phase oxidation occurs for cases 4 and 5, thus both the oxidation of gas phase and soot particles are important. That is, the model predicts that there are operating conditions where the gas phase oxidation of the precursors and growth species can have significant impact on the net soot yield.

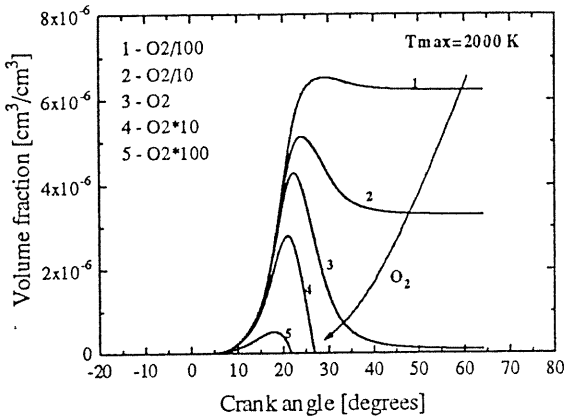

Figure 9. Predicted volume fraction versus crank angle for different oxygen concentrations for a temperature profile witha maximum temperature of 2000 K

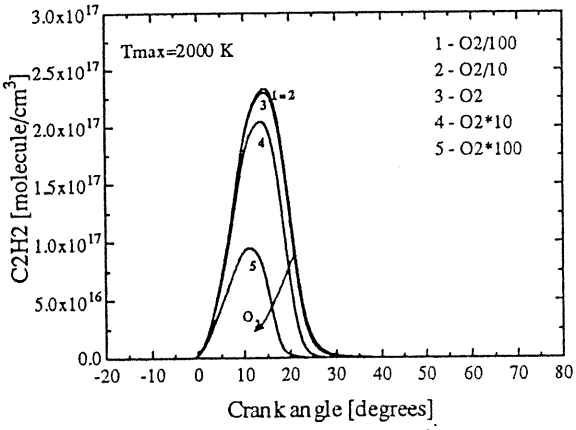

Figure 10. The effect of oxgyen concentration on the predicted growth species concentrations

Figure 11 shows the sensitivity of the net soot volume fraction to acetylene oxidation. The soot volume fraction was computed with and without the acetylene oxidation being active. The comparison shows that more soot is predicted when more acetylene is available. Thus, the final soot values depend on the balance between soot formation and oxidation processes of both solid and gas phases.

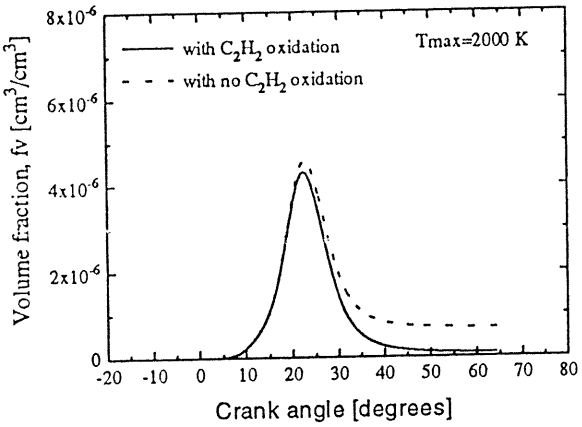

Figure 11. Predicted effect of gas phase growth species oxidation on soot volume fraction for a temperature profile with a peak temperature of 2000 K

Fuel Dependence

Figure 12 shows the net soot volume fraction when the fuel profile was varied by a factor of ten below and above the base case. Soot volume fraction shows a strong sensitivity with fuel concentration. In fact, at the lowest fuel concentration the soot oxidation is more effective then the soot formation process. In contrast, at the highest fuel concentration the soot formation process is strong enough that the balance between formation and oxidation is in favor of the soot formation process.

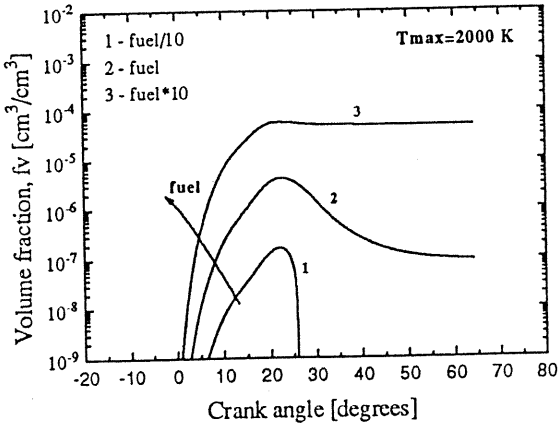

Figure 12. The effect of fule concentration on the predicted soot volume fraction with a temperature profile which has a peak temperature of 2000 K

Influence of Number of Carbon Atoms in the Fuel Molecules

Figure 13 shows the net soot volume fraction when the number of carbon atoms in the fuel was varied from 8 to 16. The soot volume fraction is predicted to increase with increasing size of the hydrocarbon fuel molecule. This results from the assumption within the model that both acetylene and precursor radicals are proportional to the number of carbon atoms in the fuel. Again, for all calculations presented up to this point in the paper, the number of carbon atoms was chosen to be 14 consistent with the tetradecane fuel used for KIVA-II simulations.

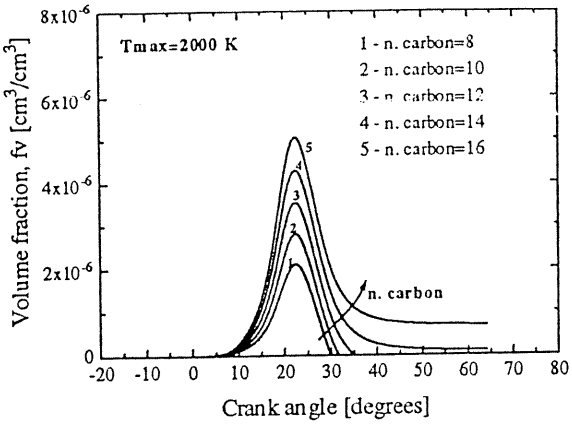

Figure 13. The effect of the number of carbon atoms in the fuel on the predicted soot volume fraction

CONCLUSIONS

This paper has presented the results of a phenomenological soot model which has been constructed for the purpose of being used as a sub-model in a larger diesel engine simulation program. The soot sub-model is a stand alone entity and includes the physical processes of inception, surface growth, coagulation and oxidation using global rate expressions. The model has been exercised by applying a set of inputs of temperature, oxygen and fuel concentration derived from the history of a typical computational cell from a KIVA II diesel simulation. The model correctly predicts the same trends observed in the literature for soot volume fraction, precursor and growth species concentration, number density and mean diameter.

REFERENCES

1. Smith, O. I., "Fundamentals of Soot Formation in Flames With Application to Diesel Engine Particulate Emissions", Prog. Energy Comb. Sci., vol. 7, pp. 275-291, 1981.
2. Haynes, B. S., and Wagner, H. Gg., "Soot Formation", Prog. Energy Comb. Sci., vol. 7, pp. 229-273, 1981.
3. Wagner, H. Gg., "Soot Formation in Combustion", Seventeenth Symposium (Int.) on Combustion, The Combustion Institute, Pittsburgh, pp. 3, 1979.
4. Hiroyasu, H., "Diesel Engine Combustion and Its Modeling", Comodia 85 Symposium, 1985.
5. Zellat, M., Rolland, Th., and Poplow, F., "Three Dimensional Modeling of Combustion and Soot Formation in an Inject Injection Diesel Engine", SAE Paper 900254, 1990.
6. Tesner, P. A., Snegiriova, T. D., and Knorre, V. G., "Kinetics of Dispersed Carbon Formation", Seventeenth

Symposium (Int.) on Combustion, The Combustion Institute, Pittsburgh, pp. 253, 1971.

7. Magnussen, B. F., and Hjertager, B. H., "On Mathematical Modeling of turbulent Combustion With Special Emphasis on Soot Formation and Combustion", Sixteenth Symposium (Int.) on Combustion, The Combustion Institute, Pittsburgh, pp. 719, 1976.
8. Magnussen, B. F., Hjertager, B. H., Olsen, J. G., and Bhaduri, D., "Effects of Turbulent Structure and Local Concentrations on Soot Formation and Combustion in C_2H_2 Diffusion Flames", Seventeenth Symposium (Int.) on Combustion, The Combustion Institute, Pittsburgh, pp. 1383, 1978.
9. Belardini, P., Bertoli, C., Del Giacomo, N., and Iorio, B., "Soot Formation and Oxidation in a DI Diesel Engine: A Comparison Between Measurements and Three Dimensional Computation," SAE Paper 932658, 1993.
10. Leung, K. M., Lindstedt, R. P., and Jones, W. P., "A Simplified Reaction Mechanism for Soot Formation in Non premixed Flames", Comb. and Flame, vol. 87, pp. 289, 1991.
11. Nishida, K. and Hiroyasu, H., "Simplified Three-Dimensional Modeling of Mixture Formation and Combustion in a D.I. Diesel Engine", SAE Paper 890269, 1989.
12. Yoshizaki, T., Nishida, K., and Hiroyasu, H., "Approach to Low NOx and Smoke Emission Engines by Using Phenomenological Simulation", SAE Paper 930612, 1993.
13. Belardini, P., Bertoli, C., Ciajolo, A., D'Anna, A., and Del Giacomo, N., "Three-Dimensional Calculations of DI Diesel Engine Combustion and Comparison With In Cylinder Sampling Valve Data", SAE Paper 922225, 1992.
14. Nagle, J., and Strickland-Constable, R. F., "Oxidation of Carbon Between 1000-2000 ^oC", Proceedings of The Fifth Conference on Carbon, Pergamon, London, pp. 154, 1962.
15. Patterson, M., Kong, S.-C., Hampson, G. and Reitz, R.D., "Modeling the Effects of Fuel Injection Characteristics on diesel Engine Soot and NOx Emissions," SAE 950523
16. Gorokhovski, M., and Borghi, R., "Numerical Simulation of Soot Formation and Oxidation in Diesel Engines", SAE Paper 930075, 1993.
17. Halstead, M.P., Kirsh, L.J. and Quinn, C.P., "Autoignition of Hydrocarbon Fuels at High Temperatures and Pressures-Fitting of a Mathematical Model," Combustion and Flame, vol. 30, pp. 45, (1977)
18. Kadota, T., and Heinein, N. A., "Time-Resolved Soot Particulates in Diesel Spray Combustion", in Particulate Carbon (D.C. Siegla and G.W. Smith, Eds.), pp. 391, 1981.
19. Bohm, H., Feldermann, Chr., Heideermann, Th., Jander, H., Luers, B., and Wagner, H.Gg., "Soot Formation in Premixed C_2H_4-Air Flames for Pressures up to 100 bar" Twenty-Fourth Symposium (Int.) on Combustion, The Combustion Institute, Pittsburgh, pp. 991, 1992.
20. Smith, G.W., "A Simple Nucleation/Depletion Model for the Spherule Size of Particulate Carbon", Comb. and Flame, vol. 48, pp. 265, 1982.
21. Prado, G., and Lahaye, J., "Physical Aspects of Nucleation and Growth of Soot Particles", in Particulate Carbon (D.C. Siegla and G.W. Smith, Eds.), pp. 143, 1981.

APPENDIX A

Table A1

Soot model variables and Differential Equations

Variable	Rate Equation
N, Soot number density (cm^{-3})	$dN/dt = N_A(r_5-r_8)$
R, precursor radical density, (mol cm^{-3})	$dR/dt = r_1-r_3-r_5$
C_2H_2, growth species density, (mol cm^{-3})	$d[C_2H_2]/dt = r_2-r_4-r_6$
f_v, soot volume fraction	$d(f_v)/dt = 1/\rho_s(r_5M_R + r_6M_C - r_7M_C)$

Where: NA = Avagadros number
MC = molecular weight of carbon
MR = mole. wt. of radical precursor

Table A2

Processes, Chemical Reactions, Rates of Reactions, Activation Energies and Pre-exponential Factors used in the Soot Model.

Process (i)	Chemical Reaction	Rate of Reaction, r_i	E_i [cal/mol]	A_i [mol cm s]
(1) Radical formation	C_mH_n ——> m/2 R	$r_1 = m/2\ A_1 \exp(-E_1/RT)$ [fuel]	120,000	0.7×10^{12}
(2) C_2H_2 formation	C_mH_n ——> m/2 C_2H_2	$r_2 = m/2\ A_2 \exp(-E_2/RT)$ [fuel]	49,000	2×10^{8}
(3) Radical oxidation	R + O_2 ——> products	$r_3 = A_3 \exp(-E_3/RT)$ [R][O_2]	40,000	1×10^{12}
(4) C_2H_2 oxidation	$C_2H_2 + O_2$ --> 2CO + H_2	$r_4 = A_4 \exp(-E_4/RT)$ [C_2H_2] [O_2]	50,000	6×10^{13}
(5) Particle inception	R ——> P	$r_5 = A_5 \exp(-E_5/RT)$[R]	50,000	1×10^{10}
(6) Particle growth	P + C_2H_2 ——> P	$r_6 = A_6 \exp(-E_6/RT)$ [C_2H_2] $S^{1/2}$ where $S = p\,D^2\,N$, $D \equiv 25$ nm	12,000	4.2×10^{4}
(7) Particle oxidation	P +O_2 ----> P	$r_7 = \left[\left(\frac{k_A P_{O_2}}{1+k_Z P_{O_2}}\right)x + k_B P_{O_2}(1-x)\right]S$ where $x = \left\{1+\frac{k_T}{k_B P_{O_2}}\right\}^{-1}$		
		$k_A = 20 \exp(-E_A/RT)$ (g-atom $cm^{-2}\,s^{-1}\,atm^{-1}$)	30,000	
		$k_B = 4.46\times10^{-3} \exp(-E_B/RT)$ (g-atom $cm^{-2}\,s^{-1}\,atm^{-1}$)	15,200	
		$k_T = 1.51\times10^{5} \exp(-E_T/RT)$ (g-atom $cm^{-2}\,s^{-1}$)	97,000	
		$k_Z = 21.3 \exp(E_Z/RT)$ (atm^{-1})	4,100	
(8) Particle coagulation	xP ——> P	$r_8 = K_{coag}\,T^{1/2}\,f_v^{1/6}\,N^{11/6}$ where $K_{coag} = 1.05\times10^{-7}$ (cm^{1}-mix $s^{-1}\,K^{-1/2}$)		